Manipulating the excitation transfer in Photosystem I by a Fabry-Perot metal resonator with optical subwavelength dimensions

Alexander Konrad,[a] Anna-Lisa Trost,[a] Sepideh Skandary,[a] Martin Hussels,[a] Alfred J. Meixner,[a] Navasard V. Karapetyan,[b] and Marc Brecht*[a,c]

[a] *Universität Tübingen, Institut für Physikalische und Theoretische Chemie, Auf der Morgenstelle 18, 72076 Tübingen, Germany. Fax: +49-7071-29-5490 ; Tel: +49-7071-29-76239; E-mail: marc.brecht@uni-tuebingen.de*
[b] *A.N. Bakh Institute of Biochemistry, Russian Academy of Sciences, Leninsky Prospect, 33, 119071 Moscow, Russia.*
[c] *Zürcher Hochschule für Angewandte Wissenschaften, Institute of Applied Mathematics and Physics, Technikumstrasse 13, 8401 Winterthur, Switzerland.*

1 Supplementary Materials

1.1 Cavity preparation

The mirrors of the resonator are composed of multiple layers deposited on 4 × 4 mm (thickness 200 μm) quartz substrate. The order of the layers is: 1 nm Cr, 30 nm (upper mirror)/60 nm Ag (lower mirror), 1 nm Au, and finally 30 nm SiO_2 (Figure 1). The final SiO_2 layer is used to exclude conformational changes

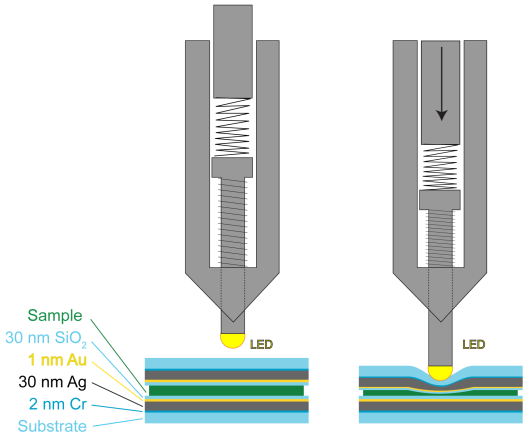

Figure 1 Scheme showing the squeezing mechanism. The cavities are formed by a sandwich of two mirrors coated with a multi-layer mirror. The squeezing is induced by a LED that is lowered (right). Note: For clarity the deformation of the upper mirror is overstated. A spring ensures that the force on the mirrors is only slightly increased.

or degradation of Photosystem I induced by contact with the metal mirrors. The layers were prepared by vapor deposition onto the quartz substrate using an electron-beam source (EB3, Edwards) under high-vacuum conditions (≈10^{-6} mbar). The film thickness was monitored during vapor deposition using an oscillating quartz unit (FTM7, Edwards) and verified by atomic force microscopy (AFM) measurements. On top of one of the mirrors less than 1μL of the sample solution (see below) was placed and then covered by the second mirror (Figure 1). This sandwich was then transfered to the sample holder designed for our low temperature transfer system (for details see Ref.[1]). This holder is fixed on the base plate of a squeezer used to produce $\lambda/2$-cavities. As shown in Figure 1, the LED is lowered to squeeze the upper mirror onto the lower mirror. The squeezing mechanism contains a spring that ensures only a slight increase of the force on the mirror during squeezing. Using a LED for squeezing features special advantages, because the curvature of the LED head can be varied to meet the requirement of the cavities and in addition, the LED serves as light source to control the formation of the Newton rings in transmission.

Figure 2a shows the side view of the squeezer constructed for the experiments. In Figure 2b, the top view of the squeezer is shown; the formation of the Newton ring pattern can be directly observed in the middle of the squeezer. Figure 2c shows a magnified image of the formed Newton ring pattern. When the inner Netwon rings belong to the first order (optical mirror distance $\lambda/2$) the squeezing process is stopped, the LED is turned off and the whole setup is plunged into a vessel filled with liquid nitrogen. The assignment of the interference orders can be done by white light transmission spectra of the resonator under a confocal microscope to determine the interference order depending on the free spectral range.

By freezing, the sample solution acts as glue holding the mirrors in the squeezed position together. The advantage of the described process is that optical glues can be avoided. This is of special advantage for biological samples, because standard sample solutions like buffer/glycerol mixtures for low temperature optical experiments can be used and the proteins are not exposed to optical glues that might damaged or at least modify the proteins. Using a home built sample transfer system enables (for details see Ref.[2]) us to transfer the squeezed sample into the cold cryostat (4.2 K) without temperature changes during handling. After mounting the sample inside the cryostat the temperature is lowered to 1.6 K.

The optical length of the cavity was determined by the white light transmission spectra as shown in Figure 3. The design

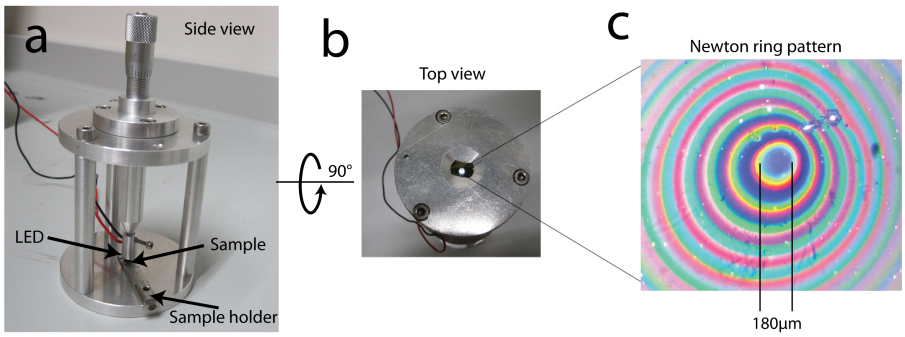

Figure 2 Squeezer for squeezing optical microcavities. (a) Side view of the squeezer. The sample holder is fixed by a screw on the base plate of the squeezer. By turning the micrometer screw, the head of the LED is lowered and squeezes the cavity. (b) Top view on the squeezer, by turning the LED on, the white light transmission through the cavity can be seen. Due to the good visibility of the Newton ring patter, the first order can be very easily adjusted with this setup. (c) Magnification of the Newton ring pattern. The inner transmission ring shows the first order of interference; here the diameter of the first order is ≈180 μm.

of our low temperature microresonator results in a mean cavity quality factor of Q ∼60 at 1.6 K, compared to Q factors of ∼30 at ambient conditions.

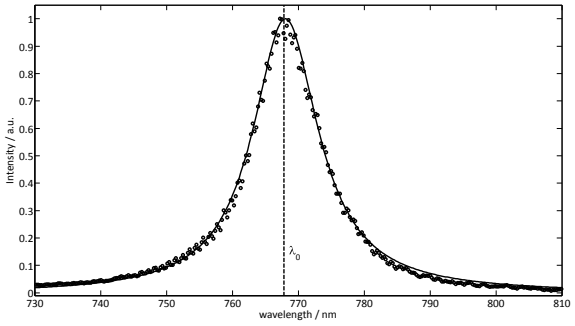

Figure 3 Microcavity white light transmission spectrum (○) fitted by a Lorentzian function (–). Resonance frequency λ_0 = 768 nm, line width 12 nm, Q = 63.

1.2 Purcell effect

According to Fermi's golden rule, the spontaneous emission rate of a two-level system depends on both, the transition dipole moment between the states and the density of modes of the electromagnetic field inside the cavity[3].

$$\Gamma_{spE} = \frac{1}{\tau_{spE}} = \frac{2\pi}{h^2} \left| \langle | \hat{\mu} \cdot \hat{E}^{+}_{cav} | \rangle \right|^2 \rho_{cav}(\omega) \qquad (1)$$

Where τ_{spE} is the lifetime of the spontaneous emission, $\hat{\mu}$ is the dipole moment of the emitter, $\hat{E}_{cav}$ is the unit-vector of the electric field of the mode with frequency ω and ρ_{cav} is the local photonic mode density of the electromagnetic field.
Dipole-like emitters undergo according to the present mode structure an enhanced or inhibited radiative relaxation. The mode structure and the subsequent modified radiative rate can be calculated according to Bjork[4]:

$$P(\lambda,L) = \Gamma_{sp}(\lambda,L)/\Gamma_{sp0} = \frac{3}{4}\int_0^{\pi/2} d\theta sin(\theta) \times \frac{(1-R)[1+R-2\sqrt{R}cos(kLcos(\theta))][1+cos^2(\theta)]}{(1-R)^2+4Rsin^2(kLcos(\theta))}. \qquad (2)$$

Here, R are the reflectivities of the resonator mirrors, Γ_{sp0} the free space radiative rate, θ is the angle of the emission due to the perpendicular axis of the plane mirrors, L is the length of the cavity in the simplified resonance condition $L = m\lambda/2$ and $k = 2\pi/\lambda$ with λ as the transmitted wavelength and m as the number of the interference order. The enhancement/inhibition factor (Purcell factor) of Γ_{sp} mirroring the wavelength depending mode distribution for a distinct cavity length.
For simulating the spectrum of an emitter i inside a given mode structure with Purcell factor $P(\lambda,L)$, the spectral band is here approximated to a Gaussian curve $\mathscr{G}_i(\lambda)$ with height A_i, peak position λ_0 and peak width w. Figure4a shows six Gaussians describing the free space spectrum of PSI from *A. platensis*, Figure4b the Purcell factor as green line for a transmission maximum of ∼740 nm. It can be seen, that on the short-wavelength side also off-axis modes with increasing θ contribute. The used objective lens (NA = 0.85) collects a variety of angular distributed resonator modes showing also off-axis emission components in the blue spectral range. For the modified spectrum $\mathscr{G}'_i(\lambda)$ the changed height $A^*_i(L)$ can be calcu-

lated by:

$$A_i^*(L) = A_i \int \mathscr{G}_i(\lambda) P(\lambda, L). \quad (3)$$

The new Gaussian $\mathscr{G}'_i$ is therefore given by:

$$\mathscr{G}'_i(\lambda, L) = A_i^*(L) e^{-(\frac{\lambda - \lambda_{0_i}}{0.5w})^2}. \quad (4)$$

Finally, the asymmetry of the Purcell factor has to be considered and all j Gaussians have to be summed up. The resulting spectrum is therefore:

$$\mathscr{G}^*(\lambda, L) = \sum_j A_i^*(L) \frac{\mathscr{G}'_i(\lambda, L) P(\lambda, L)}{\int \mathscr{G}'_i(\lambda, L) P(\lambda, L) d\lambda}. \quad (5)$$

One example spectrum is given in Figure 4b as red line. The blue line shows the measured spectrum including modifications by altered transfer dynamics inside PSI.

1.3 Confocal spectroscopy and imaging setup

Figure 5 shows the setup of our home-built confocal microscope. The microscope is mounted on a damped optical table (Opta). During measurement the sample and the microscope objective (Mikrothek 60× NA= 0.85) are immersed in liquid Helium inside a bath-cryostat (SVT-200, Janis). Temperatures below 4.2 K are generated by pumping the Helium gas with a Edwards TwoStage E2M80 combined with a Edwards EH250 booster pump. The temperature is measured close to the sample by a LakeShore Model 336 temperature controller equipped with a Cernox sensor (CX-1030-SD-HT 0.3L).
For excitation we use a fibre-coupled 665 nm *cw* diode-laser (iBEAM-660-3V2, TOPTICA Photonics). The laser is coupled into the setup using a dichroic mirror (ZQ670RDC, AHF Analysentechnik). The excitation light is then aligned along the optical axis of the microscope objective to get an optimal focus. The emitted light passes the dichroic mirror, a 30 μm pinhole, and a longpass filter (HQ 695 LP, AHF Analysentechnik) and then it can be detected by an APD (COUNT-100C, Laser Components) or a CCD-Camera (DU920P-PR-DD, Andor) mounted on a spectrograph (Shamrock 500, Andor) with 200 lines/mm and 400 lines/mm gratings. The different detectors for the emission light are selected by computer-controlled flip-mirrors. For data acquisition of the APD signals a National Instruments NI6601 counter board and a Becker & Hickl TCSPC-module (SPC-130) are used. The white light illumination is done by a white light LED. The head of the LED has a diameter of 3 mm, the radiation angle is 15°. The light of the LED is focussed on the cavity inside the cryostat by a 2″ lens with f = 60 mm as shown on the left of Figure 5.
The whole setup is controlled by a self-developed LabVIEW software. The software controls all components described above. The special aim of the software is to simplify the acquisition of high resolution spectroscopic data in fluorescence emission and white light transmission mode.

1.4 Photosystem I preparation

Trimeric Photosystem I complexes have been isolated from the cyanobacterium *A. platensis* according to Ref.[5]. Purified complexes at a concentration of about 200 μM Chl were stored in 50 mM Tris-HCl buffer (pH 8.0) and 0.08 mM (0.04% w/v) detergent n-dodecyl β-D-maltoside (Sigma) at -80 °C. For fluorescence measurements, the sample was diluted in buffer solution containing 20 mM Tricine, 25 mM $MgCl_2$ and 0.4 mM (0.02% w/v) detergent n-dodecyl β-D-maltoside (Sigma) and 5 mM sodium ascorbate for prereduction of P700 to a concentration of about 20 μM Chl. In further steps the sample was further diluted in buffer solution. In a last step glycerol was added (66% glycerol w/w). Sample preparation was carried out under indirect daylight. Several seconds before plunging the sample in liquid nitrogen, the LED used for squeezing was switched off. Due to preparation, the low temperature and the used excitation intensity, PSI is most of the time in the oxidized P700 state; for further details see Refs.[6,7]

References

[1] M. Hussels, A. Konrad and M. Brecht, *Review of Scientific Instruments*, 2012, **83**, 123706.

[2] M. Hussels, J. B. Nieder, C. Elssser and M. Brecht, *Acta Physica Polonica A*, 2012, **122**, 269–274.

[3] E. Fermi, *Rev. Mod. Phys.*, 1932, **4**, 88–132.

[4] G. Bjork, *IEEE Journal of Quantum Electronics*, 1994, **30**, 2314–2318.

[5] E. Schlodder, M. Cetin, M. Byrdin, I. V. Terekhova and N. V. Karapetyan, *Biochimica et Biophysica Acta*, 2005, **1706**, 53–67.

[6] E. Schlodder, M. Hussels, M. Cetin, N. V. Karapetyan and M. Brecht, *Biochimica et biophysica Acta*, 2011, **1807**, 1423–31.

[7] M. Brecht, M. Hussels, J. B. Nieder, H. Fang and C. Elsässer, *Chem. Phys.*, 2012, **406**, 15 – 20.

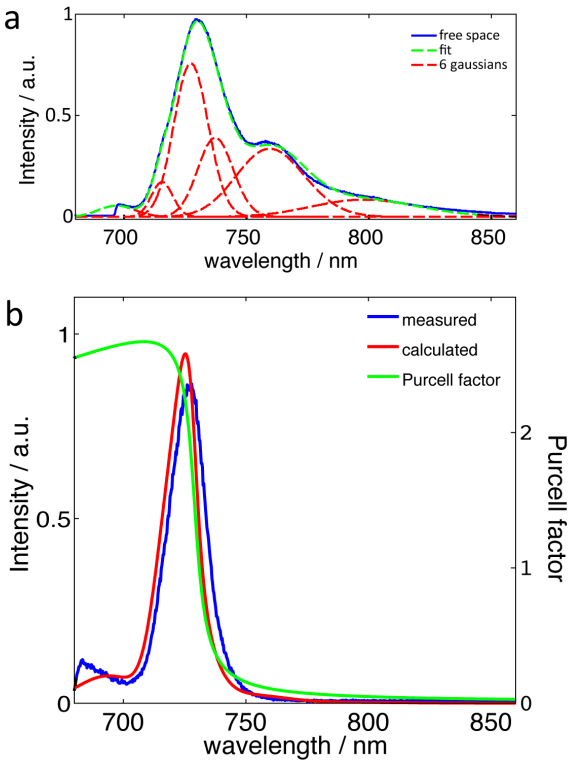

Figure 4 a) Free space spectrum of PSI from *A. platensis* (blue curve) together with a fit (green dotted curve) based on six individual Gaussian functions (red dotted curves). b) Calculated Purcell factor (green) by Eq.2 for transmission maximum of 740 nm. Also shown in red the calculated spectrum for the six Gaussians a) by Eq.3-4 and in blue the corresponding measured spectrum.

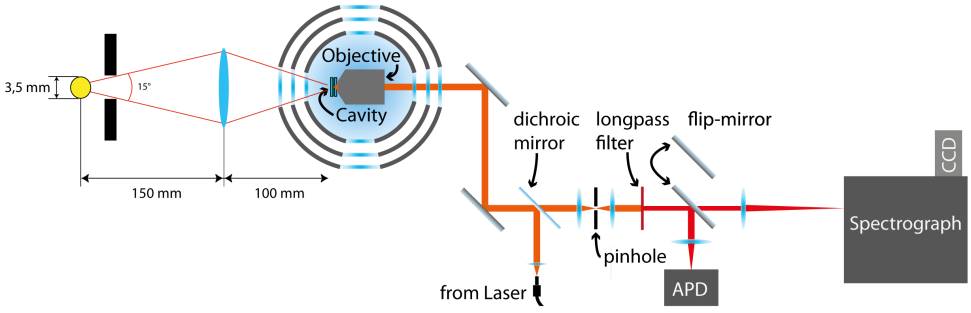

Figure 5 Scheme of the setup used for low temperature confocal spectroscopy and imaging. The details of the setup are given in the text. On the left side of the cryostat a white light LED is mounted. The light of the LED is focussed onto the cavity/sample by a 2″lens. In this arrangement the fluorescence and the white light transmission spectra can be recored by the same optical path.